Hall Effect Measurements on New Thermoelectric Materials

Jarrod Short[†], Sim Loo[†], Sangeeta Lal[†], Kuei Fang Hsu[‡], Eric Quarez[‡],
Mercouri G. Kanatzidis[‡], Timothy P. Hogan[†]
[†]Electrical and Computer Engineering Department, Michigan State University
2120 Engineering Building, East Lansing, MI 48824-1226
[‡]Chemistry Department, Michigan State University
East Lansing, MI 48824-1322

ABSTRACT

In the field of thermoelectrics, the figure of merit of new materials is based on the electrical conductivity, thermoelectric power, and thermal conductivity of the sample, however additional insight is gained through knowledge of the carrier concentrations and mobility in the materials. The figure of merit is commonly related to the material properties through the B factor which is directly dependent on the mobility of the carriers as well as the effective mass.

To gain additional insight on the new materials of interest for thermoelectric applications, a Hall Effect system has been developed for measuring the temperature dependent carrier concentrations and mobilities. In this paper, the measurement system will be described, and recent results for several new materials will be presented.

INTRODUCTION

The efficiency of thermoelectric generators is well known to be dependent on the electrical conductivity, thermoelectric power, and thermal conductivity of the materials forming the *n*- and *p*- legs of the module. Analysis of thermoelectric materials based on a one band model [1] shows the importance and interrelationship of the electrical conductivity, thermoelectric power, and the electronic contribution to the thermal conductivity. It also shows the relationship between these material parameters and the position of the Fermi energy level relative to the band edge. Based on these formulae, more information can be extracted from the data by adding the measurement of Hall effect, and determining the carrier concentration. The electrical conductivity for the one-band model for the conduction band (*n*-type materials) gives

$$\sigma = q\mu_x n = \frac{q\mu_x}{2\pi^2}\left(\frac{2k_B T}{\hbar^2}\right)^{3/2}\left(m_n^*\right)^{3/2} F_{1/2} \qquad (1)$$

where μ_x is the mobility in the x direction, m_n^* is the density of states effective mass, k_B is Boltzmann's constant (8.616×10^{-5} eV/K), T is temperature, $\hbar$, is Plank's reduced

constant, q is the electronic charge (1.602×10^{-19} C), and $F_{1/2}$ is the Fermi-Dirac function of order ½. The Fermi-Dirac function is defined as:

$$F_i = F_i\left(\zeta^*\right) = \int_0^\infty \frac{x^i}{e^{\left(x-\zeta^*\right)}+1}\,dx \tag{2}$$

and $\zeta^* = \dfrac{\zeta}{k_B T}$ is the reduced chemical potential relative to the conduction band edge.

From (1) it is also seen that the carrier concentration can be written as

$$n = \frac{1}{2\pi^2}\left(\frac{2k_B T}{\hbar^2}\right)^{3/2}\left(m_n^*\right)^{3/2} F_{1/2}. \tag{3}$$

The thermoelectric power (absolute Seebeck coefficient) for this *n*-type material is given by

$$S = -\frac{k_B}{q}\left(\frac{(s+2)}{(s+1)}\frac{F_{s+1}}{F_s} - \zeta^*\right), \tag{4}$$

and the thermal conductivity consists of an electronic contribution, κ_e, and a lattice contribution, κ_L as

$$\begin{aligned}\kappa &= \kappa_e + \kappa_L \\ &= \frac{k_B \mu_x \hbar^2}{q 4\pi^2}\left(\frac{2k_B T}{\hbar^2}\right)^{5/2}\left(m_n^*\right)^{3/2} F_{1/2}\left[\frac{(s+3)F_{(s+2)}}{(s+1)F_s} - \frac{(s+2)^2 F_{s+1}^2}{(s+1)^2 F_s^2}\right] + \kappa_L\end{aligned} \tag{5}$$

where *s* is the scattering parameter. For lattice scattering in a non-polar material $s = 0$, in a polar material $s = ½$, and for ionized impurity scattering $s = 2$. For a given value of *s*, (4) shows that the position of the reduced chemical potential relative to the conduction band edge can be determined. When the result of this is used in (3) to calculate $F_{1/2}$ the measured carrier concentration can be used to calculate the effective mass, m_n^*. The measured carrier concentration can also be used for calculating the mobility, μ_x from equation (1). The combination of these values can then be used in (5) for determining the electronic contribution to the thermal conductivity.

This shows that the Hall effect measurement is of significant importance and utility toward a more thorough understanding of the material parameters.

EXPERIMENTAL

A Hall Effect System has been developed to obtain parameters that can provide further insight into understanding new thermoelectric materials. The system provides parameters of electrical conductivity, mobility and carrier concentration. The system can test two samples during each run and collect data over a temperature range of 80-400K. The magnetic field is set up with an electromagnet that is also computer controlled up to 6000 gauss.

Samples have been prepared in the recommended manner [2] to account for undesired effects that arise due to temperature gradients and misalignment of electrical contacts made to the test specimen. Measurements are taken in four configurations of the electrical current and magnetic field as indicated in Figure 1. The measured values are then combined as:

$$V_H = \frac{V_{AB}\left(B^+, I^+\right) + V_{AB}\left(B^+, I^-\right) - V_{AB}\left(B^-, I^+\right) - V_{AB}\left(B^-, I^-\right)}{4} \qquad (6)$$

One mil diameter copper wires (0.001") were used for electrical connections and either indium soldered or silver pasted to the sample.

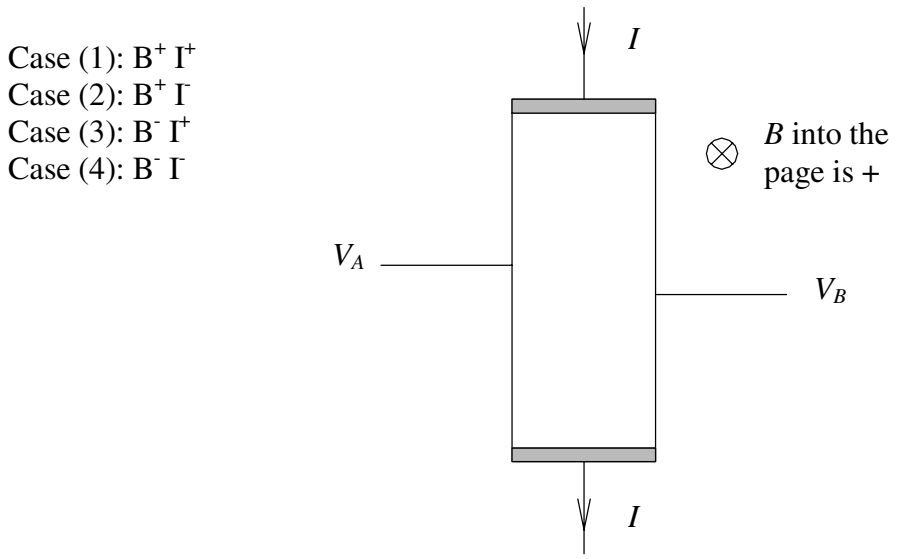

Figure 1. Configuration for Hall effect measurements. The positive directions for the current flow and magnetic field are defined in the figure.

When there is some misalignment of the Hall probes (labeled as V_A and V_B in Figure 1, the voltage measured will consist of a Hall voltage and a voltage caused by the electrical

conductivity of the sample, V_σ. The Hall voltage can be extracted from the measurements by eliminating V_σ through equation (6) as described below:
Using measurement from the four cases described in Figure 1, the measured voltages are

Case 1: $B^+ I^+$ $\quad V_{AB}\left(B^+, I^+\right) = V_\sigma + V_{H1}$

Case 2: $B^- I^+$ $\quad V_{AB}\left(B^-, I^+\right) = V_\sigma - V_{H1}$

$$V_{H1} = \frac{V_{AB}\left(B^+, I^+\right) - V_{AB}\left(B^-, I^+\right)}{2} = \frac{\left(V_\sigma + V_{H1}\right) - \left(V_\sigma - V_{H1}\right)}{2} \tag{7}$$

Likewise, if the current is reversed:

Case 3: $B^+ I^-$ $\quad V_{AB}\left(B^+, I^-\right) = -V_\sigma + V_{H2}$

Case 4: $B^- I^-$ $\quad V_{AB}\left(B^-, I^-\right) = -V_\sigma - V_{H2}$

And,

$$V_{H2} = \frac{V_{AB}\left(B^+, I^-\right) - V_{AB}\left(B^-, I^-\right)}{2} = \frac{\left(-V_\sigma + V_{H2}\right) - \left(-V_\sigma - V_{H2}\right)}{2} \tag{8}$$

Averaging the results, the Hall voltage is determined.

$$V_H = \frac{V_{H1} + V_{H2}}{2} \tag{9}$$

SYSTEM CHARACTERIZATION

The Hall effect system has been calibrated by testing reference samples for electrical conductivity, mobility and carrier concentration over the temperature range of 80-400K. For electrical conductivity, references include stainless steel, purchased and certified from the National Institute of Standards and Technology, Nickel (6N pure), bismuth (6N pure),indium antimonide ($n = 6.2\times10^{14}$). InSb and bismuth were also used to verify mobility and carrier concentrations, and tested under a 0.58 T magnetic field. For electrical conductivity, stainless steel was tested and compared with NIST data with less than 4 percent error. Bismuth and InSb were also tested, with the InSb sample having a carrier concentration similar to that found in the literature [3], and [6]. Bismuth was also tested with good agreement to the literature [5]. Reference data for InSb and Bi were extracted from plots, so the actual values are not known precisely. Although the measured and reference data show to match well, this attributes to slight deviation when comparing results.

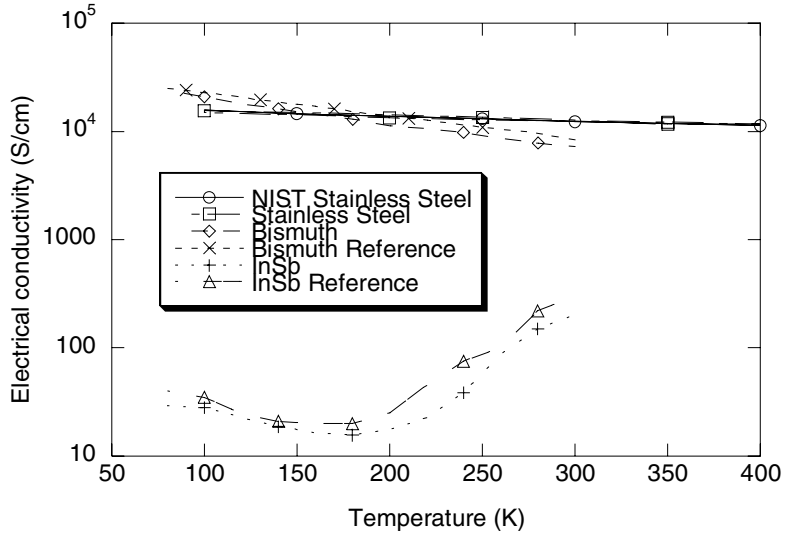

Figure 2. Electrical conductivity vs. temperature for stainless steel, bismuth, and InSb samples.

The mobility of InSb and Bi samples were determined from the Hall coefficient and electrical conductivity measurements as shown in Figure 3.

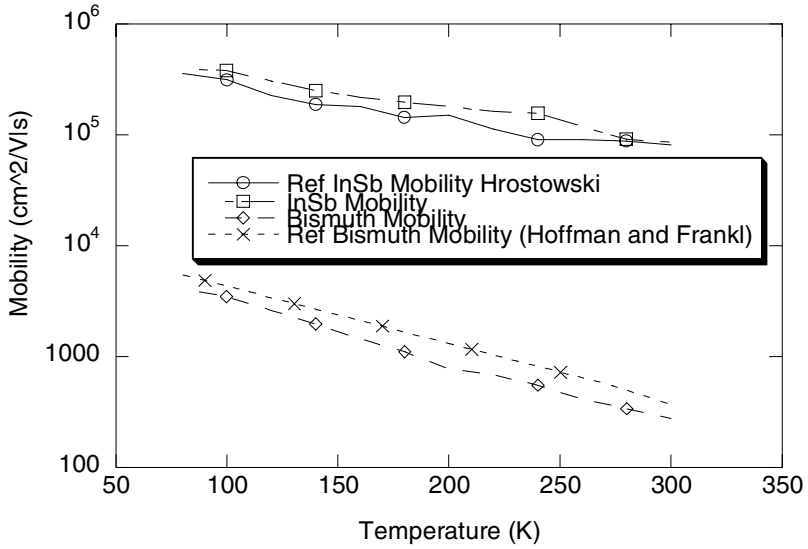

Figure 3. Mobility of InSb and Bi as a function of temperature.

Finally, carrier concentrations are compared for InSb and Bi to the literature values. The reference data taken for InSb shows the same trend, however the doping concentration is slightly different from that of the reference data.

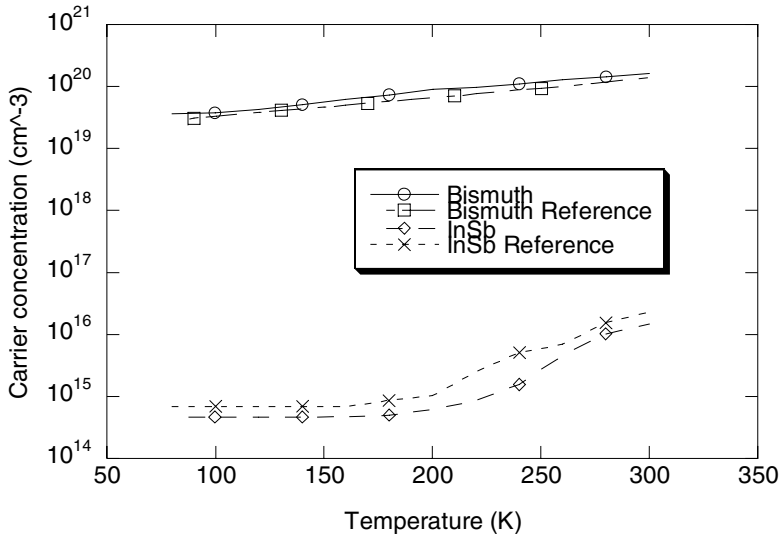

Figure 4. Carrier concentrations for Bi and InSb as determined from measured Hall effect data.

NEW THERMOELECTRIC MATERIALS

New thermoelectric materials composed of Ag-Pb-Te-Sb have also been characterized. A separate system [4] that yields thermopower, thermal conductivity, and electrical conductivity was also utilized for these samples. The electrical conductivity, mobility, and carrier concentrations are shown in Figures 5, 6 and 7.

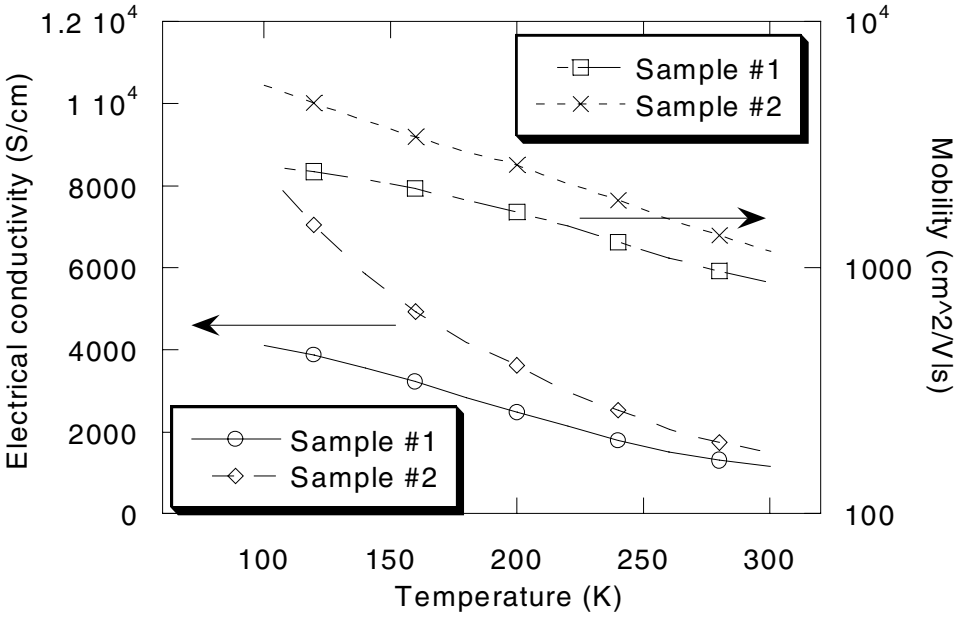

Figure 5. Electrical conductivity and mobility for two different samples of Pb-Sb-Ag-Te.

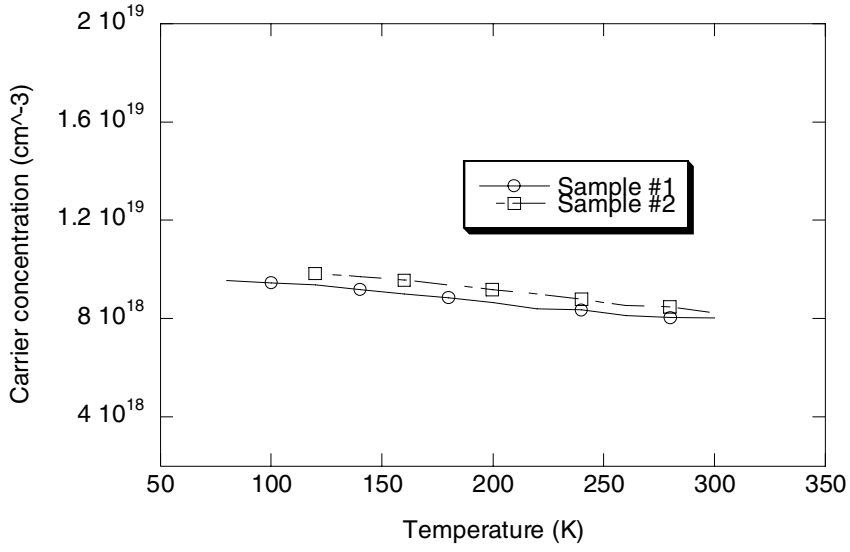

Figure 6. Carrier concentrations for the samples shown in Figure 5.

The electrical conductivity, and thermopower for Sample #1 were also measured on a separate system, and found to be in very good agreement as shown in Figure 7.

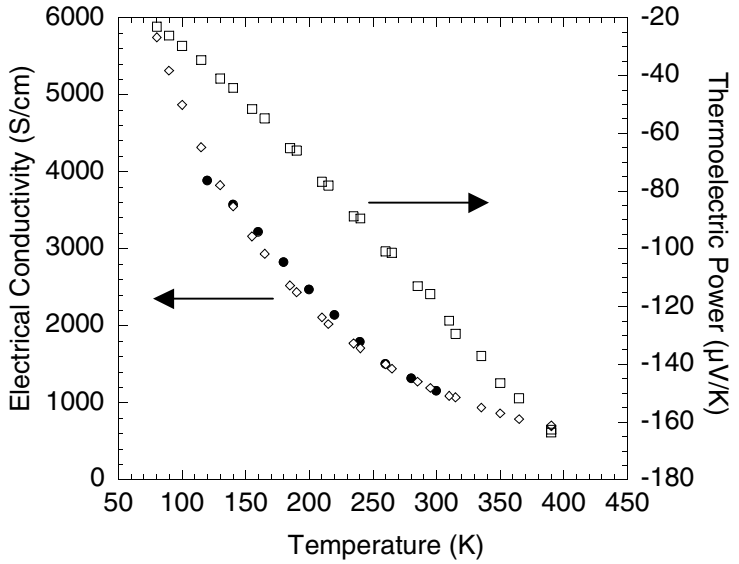

Figure 7. Electrical conductivity and thermoelectric power for Sample #1 shown in Figure 5.

By finding the Fermi-Dirac integrals of order ½ through numerical integration, the measured thermoelectric power can be used to determine the position of the reduced chemical potential as a function of temperature through equation (4). A plot of equation (4) as a function of reduced chemical potential is shown in Figure for scattering parameters of 0, ½, and 1.

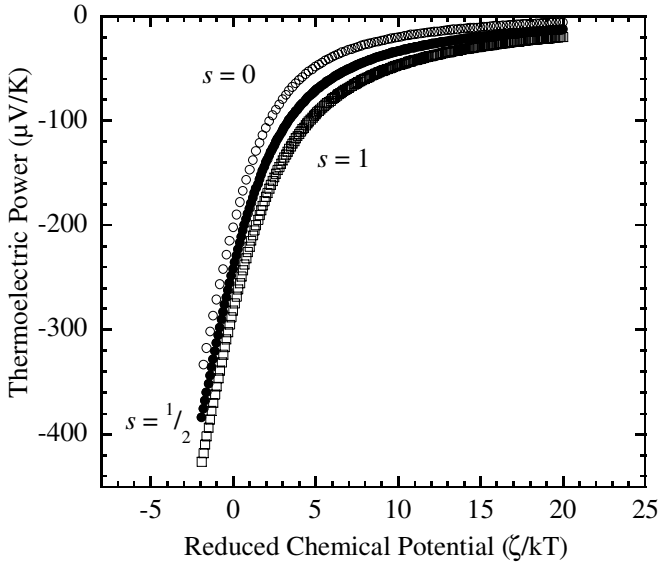

Figure 8. Calculated thermoelectric power as a function of ζ^*.

From this plot, and the measured data of Figure 7, ζ^* can be found as a function of temperature.

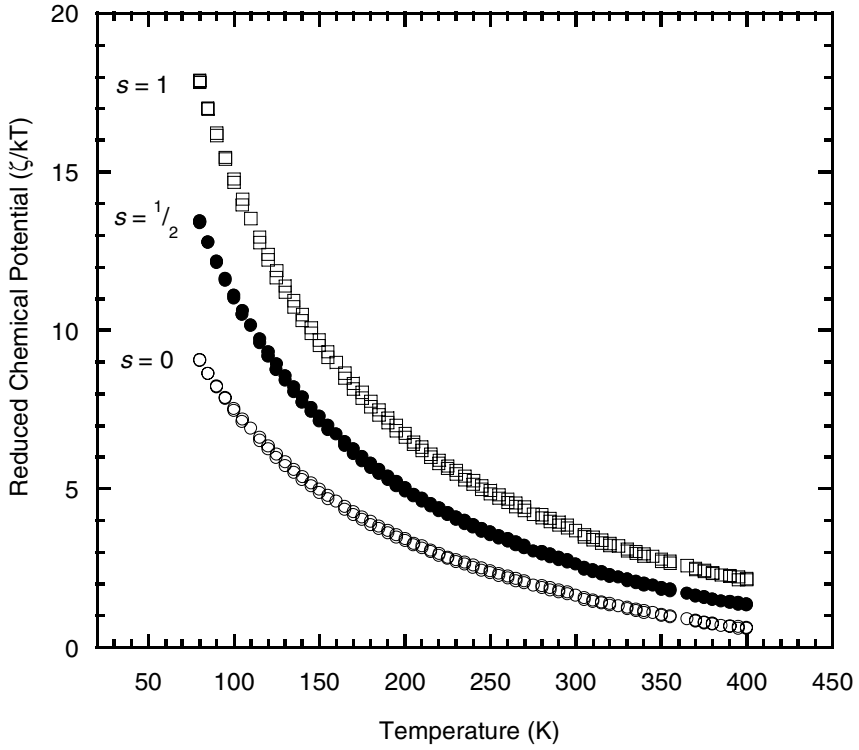

Figure 9. Reduced chemical potential vs. temperature based on equation (4) and the measured thermopower data in Figure 7.

The density of states effective masses calculated for the three scattering cases are shown in Table 1 for T = 300K, and are comparable or slightly larger than the value for PbTe ($0.17m_o$) [7].

Table (1): Effective Mass Calculations for T=300K

		Sample #1
Case 1: s=1	ζ^*	3.684
	$\mathbf{F_{1/2}}$	5.172
	m*	$0.147m_o$
Case 2: s=½	ζ^*	2.628
	$\mathbf{F_{1/2}}$	3.389
	m*	$0.195m_o$
Case 3: s=0	ζ^*	1.641
	$\mathbf{F_{1/2}}$	2.061
	m*	$0.272m_o$

CONCLUSIONS

The use of Hall effect measurements in the analysis of heavily doped semiconductors, such as those commonly used in thermoelectrics, is of great benefit toward a better understanding of the fundamental material properties. Results from a new Hall effect system for reference samples, and some new chalcogenide based materials has been shown.

ACKNOWLEDGEMENT

This research was possible through the gracious support of the Office of Naval Research (ONR).

REFERENCES

1. L. D. Hicks, M. S. Dresselhaus, "Effect of Quantum-Well Structures on the Thermoelectric Figure of Merit", *Physical Review B*, Vol. 47, No. 19, pp. 12727-12731, 1993.
2. E. H. Putley, *The Hall Effect and Semi-conductor Physics*, (1960).
3. H. J. Hrostowski, F. J. Morin, T. H. Geballe, and G. H. Wheatley, "Hall Effect and Conductivity of InSb", *Physical Review B*, Vol. 100, No. 6, 1672-1676, 1955.
4. T. Hogan, N. Ghelani, S. Loo, S. Sportouch, S.-J. Kim, D.-Y. Chung, M. G. Kanatzidis, "Measurement System for Doping and Alloying Trends in New Thermoelectric Materials," *Eighteenth International Conference on Thermoelectrics Proceedings*, pp. 671-674, 1999.
5. R. A. Hoffman and D. R. Frankl, "Electrical Transport Properties of Thin Bismuth Films*", *Physical Review B,* Vol. 3, No. 6, 1825-1833, 1971.
6. D. L. Rode, "Electron Transport in InSb, InAs, and InP", *Physical Review B*, Vol. 3, No. 10, 3287-3299, 1970.
7. B. G. Streetman and S. Banerjee, *Solid State Electronic Devices,* Prentice Hall, Upper Saddle River, NJ, (2000).